Carbon Nanotube/Isotactic Polypropylene Composites Prepared by Latex Technology: Morphology Analysis of CNT-Induced Nucleation

Kangbo Lu,[†,‡] Nadia Grossiord,[‡,§] Cor E. Koning,[‡,§,||] Hans E. Miltner,[||] Bruno van Mele,[||] and Joachim Loos*[,†,‡,⊥]

Laboratory of Materials and Interface Chemistry, and Soft Matter Cryo-TEM Research Unit, Eindhoven University of Technology, P.O. Box 513, 5600 MB Eindhoven, The Netherlands, Dutch Polymer Institute, P.O. Box 902, 5600 AX Eindhoven, The Netherlands, Laboratory of Polymer Chemistry, Eindhoven University of Technology, P.O. Box 513, 5600 MB Eindhoven, The Netherlands, Physical Chemistry and Polymer Science and FCOL (CEK), Vrije Universiteit Brussel, Pleinlaan 2, B-1050 Brussels, Belgium, and Laboratory of Polymer Technology, Eindhoven University of Technology, P.O. Box 513, 5600 MB Eindhoven, The Netherlands

Received April 14, 2008; Revised Manuscript Received August 24, 2008

ABSTRACT: The crystallization behavior of isotactic polypropylene (iPP) in the vicinity of single-wall and multiwall carbon nanotubes (SWCNTs and MWCNTs) has been studied. Combined DSC and transmission electron microscopy (TEM) investigations of bulk composite materials reveal that CNTs nucleate iPP when crystallizing from the quiescent melt and that iPP crystals form a transcrystalline layer of aligned iPP lamellar crystals around the nucleating CNT. The pronounced nucleation effect and the formation of a transcrystalline layer is observed also for ultrathin film CNT/iPP samples. Corresponding diffraction studies show that in bulk as well as in the case of the ultrathin film samples only the α-phase of iPP exists. The transcrystalline layer is highly oriented around the nucleating CNTs, and the crystallographic *c*-axes of the lamellae are oriented perpendicular to the long axis of the nucleating CNT, which is in contradiction to assumptions done in other studies. This crystallization behavior is discussed and a possible explanation is provided based on iPP macromolecules wrapped around rather than aligned along the CNTs prior to formation of the nucleus.

Introduction

Isotactic polypropylene (iPP) is among the most extensively studied thermoplastics with widespread applications, because of its excellent properties and low price. Over the years, iPP has been reinforced with various inorganic or organic fibers (e.g., carbon, glass, Kevlar, PET, PTFE, natural fibers)[1−3] as well as other fillers (talc, mica, calcium carbonate, etc.),[4,5] essentially aiming at improving its mechanical and functional performance.

Recently, carbon nanotubes (CNTs) as a new kind of nanofiller particles have attracted a great deal of interest from all over the world since the study published by Iijima in 1991.[6] CNTs possess unique mechanical, thermal, and electrical properties, such as a high elastic modulus (which can be larger than 1 TPa), thermal stability up to 2800 °C in vacuum, thermal conductivity approximately twice as high as that of diamond, and so on.[7−10] Their unique properties and high aspect ratio make CNTs a preferred candidate to be used as fillers in manufacturing high-performance and in particular conductive composites.[11−17] A prerequisite for successful preparation of such composites, however, is the achievement of a homogeneous CNT dispersion throughout the iPP matrix.

As-produced CNTs invariably exist either as aligned aggregates or bundles, which are tightly bound by an estimated interaction of 500 eV/μm of tube length for single-wall carbon nanotubes (SWCNTs),[18,19] or are highly entangled in case of multiwall carbon nanotubes (MWCNTs). Therefore, the dispersion and incorporation of CNTs as individuals in polymer matrices is one of the most important and challenging tasks toward maximizing the translation of CNT properties to the composites. To incorporate CNTs in polymer matrices, several methods have been proposed, including melt-processing[20−22] and extrusion,[23] mechanical stretching,[24] spin coating,[25] the use of latex technology[14,26−28] or magnetic fields,[29] a coagulation method,[30] and in situ polymerization.[31−33] In recent studies, others and we have demonstrated that the latex technology successfully can be applied to prepare SWCNT/polymer and MWCNT/polymer composites.[26,27,34,35]

In the present study, we apply the latex technology for the preparation of both SWCNT/iPP and MWCNT/iPP composites with low loadings of CNTs. Besides the improved functionality of such composites, in particular their tailored conductivity, in the first paper of this series we have introduced the remarkable nucleation effect that CNTs have on iPP. On the basis of calorimetric investigations, we have studied in detail the influence of CNT loading, type of the CNT nanofillers, and the thermal pretreatment on the crystallization and melting behavior of iPP, and we found, for example, that for a SWCNT loading of 1wt % the crystallization onset temperature of the iPP rises for about 14 °C when crystallizing from the quiescent melt.[36] The molecular origin of nuclei formation at the surface of a CNT and its influence on the crystal growth behavior, however, currently are in discussion and not yet well understood.[37−40] Therefore, it is the purpose of this study to shine light on the morphological organization of iPP crystals close to nucleating CNTs, both for bulk as well as for ultrathin films.

Experimental Section

Materials. Two types of carbon nanotubes have been used in this study, both prepared by chemical vapor deposition. Thin MWCNTs commercialized under the trade name Nanocyl-3100 were obtained from Nanocyl S.A. (Belgium), whereas HiPCO SWCNTs were purchased from Carbon Nanotechnology, Inc. (USA). The carbon nanotubes were used as-received after purifica-

* Corresponding author. E-mail: j.loos@tue.nl.
[†] Laboratory of Materials and Interface Chemistry, and Soft Matter Cryo-TEM Research Unit, Eindhoven University of Technology.
[‡] Dutch Polymer Institute.
[§] Laboratory of Polymer Chemistry, Eindhoven University of Technology.
[||] Vrije Universiteit Brussel.
[⊥] Laboratory of Polymer Technology, Eindhoven University of Technology.

10.1021/ma8008299 CCC: $40.75
Published on Web 10/09/2008

tion by the supplier (impurities <5 wt % for the MCWNTs, and in the range of 10−15 wt % in the SWCNTs).

The surfactant used for the dispersion of the CNTs in water was SDS (90%) provided by Merck Chemical Co. All dispersion experiments were carried out with distilled water.

The polymer matrix material is a water-based emulsion of maleic anhydride-grafted isotactic polypropylene (iPP-g-MA, called in short iPP in this study), commercialized by Solvay S.A. (Belgium) under the trade name Priex801. It was designed for antistatic applications and contains additives, enhancing its conductivity. According to the supplier, the aqueous emulsion is composed of 25 wt % of iPP polymer and 7 wt % of anionic surfactant of the oleic acid type, neutralized by an amino-alcohol, the remainder being water. The weight-average molar mass of the polymer is in the range M_w = 50 000−60 000 g/mol with about 30 wt % of the iPP below 20 000 g/mol, as determined by GPC in trichlorobenzene using linear polyethylene standards (measured at DSM Resolve, The Netherlands).

CNT/iPP Bulk Nanocomposite Preparation. One wt % CNTs was dispersed in 1.5 wt % aqueous SDS solution driven by sonication. After the maximum degree of dispersion had been achieved according to UV−vis spectroscopy measurements,[41] the dispersion was centrifuged at 3500 rpm for 30 min, at a Varifuge RF ES3000 with a Sepatech rotor (11 cm), to remove the remaining big CNT bundles and catalyst residues. The supernatant was mixed with iPP latex, the mixture was then frozen in liquid nitrogen for several minutes, and the aqueous solvent was removed overnight with a Christ Alpha 2-4 dryer operated at 0.2 mbar and 20 °C. The resulting composite powder was compressed into films at 180 °C between poly (ethylene terephthalate) sheets with a Collin Press 300G. Detailed information on the complete preparation process can be found in refs 26−28.

Differential Scanning Calorimetry (DSC). DSC experiments were performed in either conventional or modulated mode (Modulated Temperature DSC - MTDSC) on a helium-purged TA Instruments 2920 DSC and equipped with a refrigerated cooling system (RCS). Temperature and enthalpy calibration were performed using an indium standard. Sample masses were typically in the range 3−5 mg, contained in nonhermetic aluminum crucibles (Perkin-Elmer).

CNT/iPP Ultrathin Film Model Samples. The ultrathin film samples were prepared by casting a layer of an aqueous dispersion of CNTs and iPP latex on carbon-supported TEM copper grids. The cast film samples were heated to 180 °C for 5 min, then cooled to room temperature. The applied temperature settings were similar to those for the calorimetric measurements performed by DSC.

Transmission Electron Microscopy (TEM). TEM observations of the CNT/iPP nanocomposites were performed using a Titan-Krios operated at 300 kV acceleration voltage or a Tecnai 20 G^2 operated at 200 kV (both FEI Co., The Netherlands). Ultrathin CNT/iPP model samples were investigated as prepared. For investigations of the bulk morphology of CNT/iPP samples, pieces of the as-prepared bulk composites were stained for a few hours in RuO_4 solution and subsequently cryo ultramicrotomed at −100 °C (Leica Ultracut) into cross sections with a thickness of about 80 nm, which were transferred on TEM copper grids. (*hkl*)-Indexing of the diffraction patterns obtained was performed using standard *d*-spacings and corresponding (*hkl*)-indexes of the α-phase crystal structure of isotactic polypropylene; the camera length of the microscope was calibrated using gold standard.

Results

Recently, we have performed a detailed calorimetric study on CNT/iPP composites and analyzed the CNT load-dependent crystallization and melting behavior of the iPP matrix (part one in this series of papers).[36] The main conclusion drawn from this study was that CNTs strongly nucleate the iPP when cooling the sample from the quiescent melt. As shown in Figure 1, the crystallization onset temperature of the iPP when cooled from the quiescent melt increases for low loadings of both SWCNTs and MWCNTs and approaches its maximum plateau value for loadings of about 1 wt %. The crystallization onset temperature rises about 9 °C from 122 °C for the neat iPP to 131 °C for MWCNT/iPP composites, and about 14 °C to a maximum value of 136 °C for iPP filled with SWCNTs. This remarkable effect indisputably demonstrates the high efficiency of CNTs as nucleation agent for iPP; a similar nucleation effect was investigated also in previous studies,[4,42] but the reason for this additional striking feature of CNTs and underlying physical characteristics, however, is not yet completely understood.

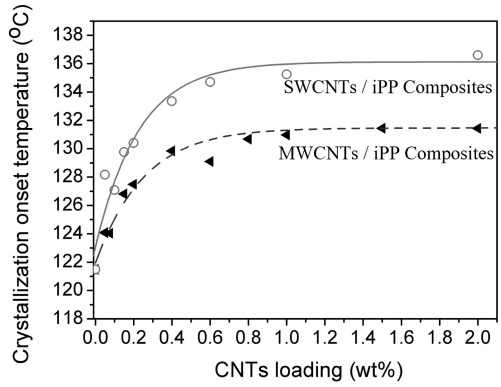

Figure 1. Plot of the iPP crystallization onset temperature of CNT/iPP composites versus their actual loading with SWCNTs (○) and MWCNTs (▲).

Figure 2 shows a series of TEM bright-field images acquired at slight underfocus conditions. All three samples under investigation are bulk samples that were cryo-microtomed to prepare ultrathin electron transparent slices. Figure 2a represents the morphology of neat iPP as obtained for the chosen crystallization conditions: after staining, the common cross-hatched organization can be seen with brighter lamellar crystals surrounded by the darker because of heavily stained amorphous material.

Following the latex-based route for the preparation of nanocomposites, as introduced above, homogeneous distribution of CNTs in any polymer latex matrix of choice can be achieved; this is the case for iPP as matrix material, too. Figure 2b shows the dark-grayish MWCNTs embedded and homogeneously distributed in the iPP matrix; the MWCNT concentration of the sample is 1 wt %. It should be noted that the sample shown in Figure 2b has not been stained so that no contrast within the iPP matrix is obtained. After a similar sample was stained with RuO_4, iPP lamellar crystals can be observed that are oriented perpendicular to a MWCNT (Figure 2c, the MWCNT is marked by the arrows) and form a transcrystalline layer. However, because of staining the sample, the good contrast of the MWCNT with the unstained polymer matrix (as displayed in Figure 2b) vanishes, and MWCNTs can hardly be recognized.

For a better understanding of the interaction between CNTs and the surrounding iPP matrix, we have performed crystallization experiments in ultrathin films of iPP and CNTs, as model systems. For this purpose, a droplet of the pure aqueous polypropylene latex dispersion or the CNT/iPP latex dispersion was deposited on an amorphous carbon-coated TEM grid, heated to 180 °C for 5 min, and subsequently cooled to room temperature so that the iPP can crystallize. Figure 3 shows TEM bright-field images in slight defocus conditions; in contrast to stained samples, in case of phase contrast imaging as applied here, the darker lines now correspond to the lamellar crystals. Again, for the neat iPP the common cross-hatched morphology is formed (Figure 3a). When the iPP is crystallized in contact with MWCNTs (Figure 3b), lamellar crystals are formed that grow perpendicular to the long axis of the MWCNTs. It is

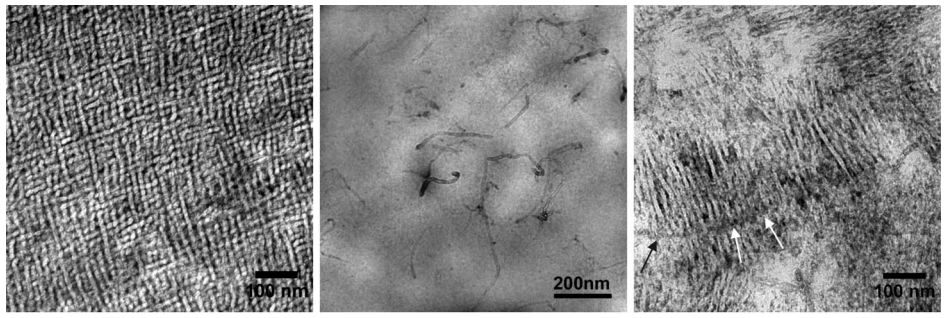

Figure 2. TEM bright-field images of bulk samples of (a) pure iPP showing characteristic cross-hatched morphology after staining with RuO_4, (b) unstained 1 wt % MWCNT/iPP composite demonstrating homogeneous dispersion of the MWCNTs, and (c) the same stained MWCNT/iPP nanocomposite showing transcrystalline grown iPP around a MWCNT (location of the MWCNT is indicated by the arrows).

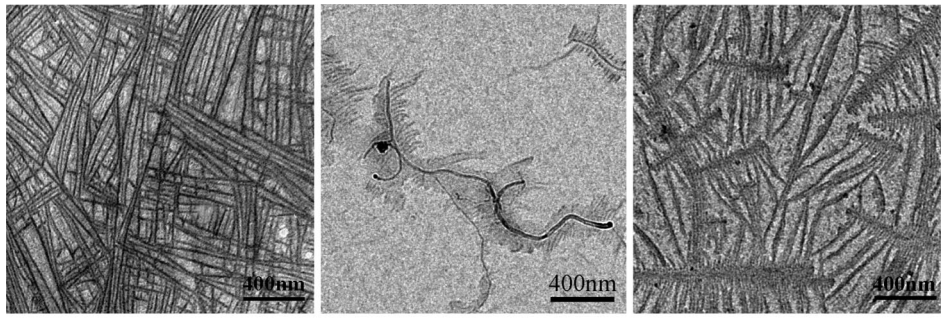

Figure 3. TEM bright-field images of ultrathin film samples of (a) pure iPP showing cross-hatched morphology; and transcrystalline organization of iPP around (b) MWCNTs and (c) SWCNTs (the SWCNTs are not visible).

obvious that the iPP crystallization is nucleated at the surface of the MWCNTs, because the perpendicular orientation of the iPP lamellae follows even narrow curvatures of the MWCNTs.

Comparing the mechanical properties of SWCNTs with MWCNTs, it is known that SWCNTs are stiffer and have a straighter appearance when deposited on a substrate. Figure 3c shows the TEM image of an ultrathin iPP film crystallized in the presence of SWCNTs. Once more, iPP lamellar crystals are grown perpendicular to the long axis of the SWCNTs. The width of the transcrystalline layer varies with the location in the sample; besides lamellae of about 100 nm in length, some very long lamellar crystals can be seen with lengths of one-half a micrometer or longer; actually, the length depends on the local available iPP material and the density of the nucleation sides. Because of their tiny diameter of about 1−2 nm and their carbon-based nature, SWCNTs cannot be detected directly by TEM when embedded in a polymer matrix, and no contrast between the SWCNTs and the surrounding polymer matrix can be achieved. From other studies, however, we know that the length of the SWCNTs being submitted to the ultrasonication procedure is often about 500−1000 nm.[26,29] It is apparent that all transcrystalline structures seen in Figure 3c have a core length (perpendicular to the growth axes of the iPP lamellae) in the same order of magnitude. This is why we believe that the central part of the transcrystalline structures is one SWCNT or most probably a cluster of a few SWCNTs that nucleates the iPP matrix material to form the transcrystalline layer. As a side aspect of this observation, we would like to mention that decoration of SWCNTs by a transcrystalline grown polymer layer is a convenient technique for the determination of the actual length of the SWCNTs. This procedure is somehow similar to the decoration technique as used for visualizing extended-chain shish crystals.[43] Consequently, the length of the SWCNTs embedded in the iPP matrix used in our experiments varies from about 300 nm to about 1 μm.

To reveal the orientation relation between the iPP lamellar crystals and the nucleating CNT, we have performed selected-area electron diffraction (SAED) experiments. Figure 4a shows the SAED pattern of pure iPP as crystallized from the melt on the carbon-coated TEM grid. The common cross-hatched morphology (Figure 3a) results in random crystal orientations of the lamellar crystals with respect to the electron beam so that all common (*hkl*)-reflections of the α-phase are present. Figure 4b,c shows the bright-field TEM image of transcrystalline grown iPP lamellae around SWCNTs and the corresponding SAED pattern of the same area. Evidently, the diffraction pattern originates from highly oriented iPP lamellar crystals nucleated along the long axis of the SWCNTs and is somewhat similar to the well-known fiber patterns of iPP. After careful inspection and indexing of the observed reflections, we can state that only (*hk*0)-reflections of the α-phase are present. The straightforward conclusion drawn from this result is that all lamellar crystals are oriented flat-on with respect to the sample substrate, and that the *c*-axis of the crystals is parallel to the electron beam. The iPP molecules are oriented tangential with respect to the short axis rather than parallel to the long axis of the SWCNT. Similar results are achieved related to the orientation of iPP lamellar crystals with respect to MWCNTs in ultrathin films (Figure 4d,e) as well as for CNT bulk samples (Figure 4f). In case of the bulk sample, the TEM specimen has a thickness of about 100 nm. On such specimen, we searched for an area where most of the lamellae are nucleated by a CNT and are grown in-plane of the specimen section, which is the only situation in which we are able to observe the lamellae. However, in the full volume of the bulk sample, the iPP lamellar crystals are grown in all radial directions after being nucleated by the CNT. Thus, we cannot prevent that also some iPP material is probed that shows crystalline orientation slightly different from that of the majority of the crystals. Moreover, we assume that for the nucleation of iPP SWCNT clusters rather than individual

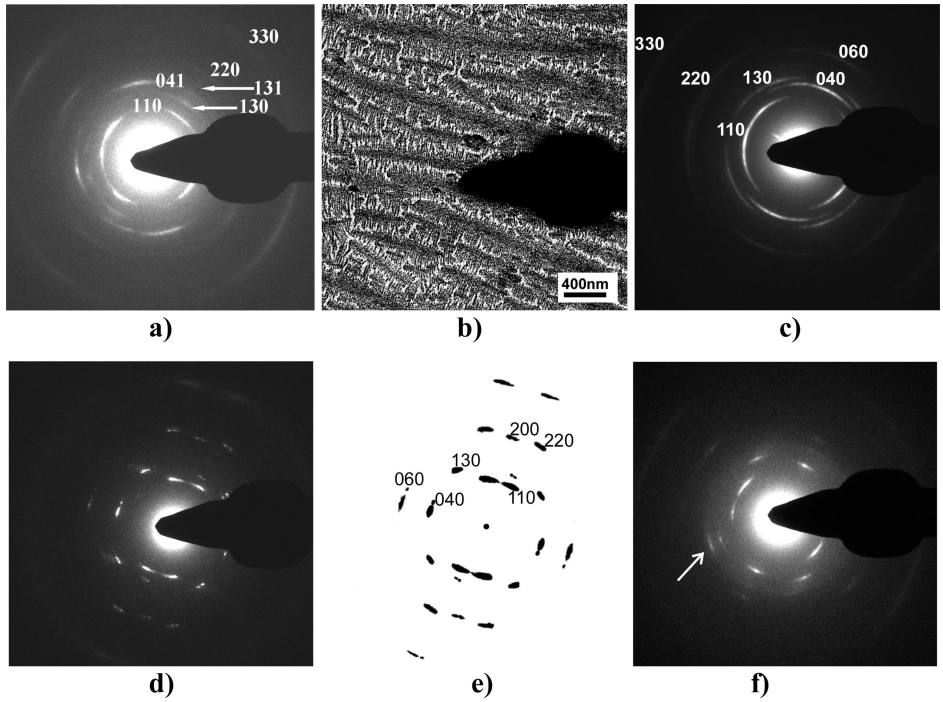

Figure 4. (a) Selected-area electron diffraction pattern of the pure iPP crystallized on the carbon-coated TEM grid (typical morphology is shown in Figure 3a), (b) bright-field TEM image and (c) corresponding SAED pattern originating from the same area of transcrystalline grown iPP around SWCNTs in an ultrathin film, (d) SAED pattern of transcrystalline grown iPP around MWCNTs, and (e) corresponding sketch indicating the (*hkl*)-indices of the Bragg-reflection; only (*hk*0) reflections are present. (f) Selected-area electron diffraction pattern of a bulk sample nucleated by a MWCNT showing an iPP crystal orientation similar to the case of the ultrathin film; however, also the (041) reflection is visible (indicated by the arrow); because the specimen originates from a bulk volume, we cannot prevent that also some iPP material is probed that shows crystalline orientation slightly different from that of the majority of the crystals nucleated by the CNT and grown in-plane of the section.

SWCNTs are responsible; only such clusters can provide the required surface size (1−2 nm for an individual SWCNT vs 5−10 nm for a small cluster) to initiate nucleation of the iPP crystals.

Discussion

Both the calorimetric as well as the morphological studies show strong evidence for a pronounced nucleation effect of SWCNTs and MWCNTs on isotactic polypropylene: the crystallization from the quiescent melt of iPP filled with CNTs starts at much higher temperatures as compared to that of the neat iPP, and the prominent formation of the transcrystalline layer of iPP around both the SWCNTs and the MWCNTs demonstrates the potential of CNTs as nucleation agents for iPP. In case of bulk CNT/iPP composites, the CNTs are well-dispersed in the iPP matrix so that the interface between CNTs and the surrounding iPP matrix is maximized, which causes for CNT concentrations as low as 1 wt % pronounced nucleation of the whole iPP matrix, for both SWCNTs as well as for MWCNTs. This also is valid for the ultrathin film experiments, for which we have adjusted the amount of CNTs such that always individual CNTs or clusters of a few SWCNTs are present in the surrounding iPP matrix. Around all CNTs, transcrystalline iPP lamellae can be found that are nucleated at the surface of the CNTs.

In our study, we only observed crystallization of iPP in the α-phase. Moreover, it is commonly expected that polymer macromolecules should adsorb along the long axis of CNTs because of local confinement of the chains at the surface of the CNT, so-called soft epitaxy,[39] and that these confined molecules form nuclei with *c*-axis orientation parallel to the long axis of the CNT. However, for the ultrathin film experiments we have performed but also for bulk samples we have investigated, the dominant *c*-axis orientation of the transcrystalline nucleated lamellar crystals is perpendicular to the long axis of the nucleating CNTs and perpendicular to the substrate plane (in case of films) as demonstrated by the selected area electron diffraction patterns obtained. Therefore, the orientation of the very first molecules, probably adsorbed at the surface of the CNTs, that induces the formation of a stable nucleus should be perpendicular rather then parallel to the long axis of the CNTs. This situation is sketched in Figure 5: iPP macromolecules are adsorbed at the surface of the CNTs in the melt and are partially wrapped around the CNTs; probably the protruding methyl groups of the iPP interact with the graphite layer of the CNT. This confinement of the macromolecules is kept during cooling of the sample from quiescent melt and causes enhanced and oriented nucleation of iPP lamellar crystals, which have their crystallographic *c*-axis tangential to the graphite shell(s) of the CNTs. From corresponding thermal analysis studies,[36,44] we can exclude any influence of the grafted maleic anhydride and the surfactant used for stabilization of both the CNT and the iPP latex dispersions on the crystallization behavior and the crystal orientation of the iPP; in particular, in ref 44 we have

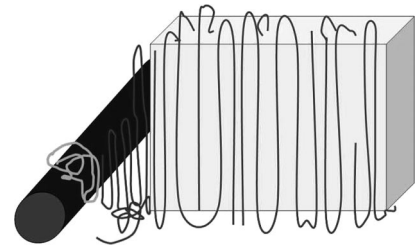

Figure 5. Sketch explaining the possible nucleation mechanism of iPP on the surface of a CNT; iPP macromolecules initially are partly wrapped around the CNT (brighter macromolecule in the sketch, dark rod represents a CNT) and form a nuclei with crystallographic *c*-axis perpendicular to the long axis of the CNT.

demonstrated that the surfactant, which coats the CNTs in dispersion, is exchanged with low molar mass polymer chains of the matrix material during thermal treatment, which certainly also happened in the CNT/iPP systems under investigation.

Conclusions

Carbon nanotubes are nanofillers that have a unique combination of attractive properties: high thermal and electrical conductivity, high strength and stiffness, and low density, to name but a few. In the present study, we have demonstrated that SWCNT and MWCNT are excellent nucleation agents for iPP, which substantially increases its crystallization temperature when cooling from the quiescent melt. The iPP matrix nucleates at the CNTs and forms a highly oriented transcrystalline layer around them, which is observed for both bulk crystallization of iPP as well as for crystallization in ultrathin film samples. In all cases, analysis of the corresponding electron diffraction patterns indicates high orientation of the iPP lamellar crystals perpendicular to the long axis of the CNTs with the *c*-axis orientation tangential to the CNT. This crystal orientation is explained by iPP macromolecules that are probably wrapped around the CNT in the melt; this confinement is kept during the nucleation process and determines the *c*-axis orientation of the lamellar crystals formed.

Acknowledgment. This study is part of the research program of the Dutch Polymer Institute (Project number #416 "A new concept for obtaining homogeneous distributions of carbon nanotubes in polymer matrices"). The work of H.E.M. was supported by a grant of the Fund for Scientific Research Flanders (FWO). H. Wautier at Solvay S.A. is kindly acknowledged for supplying the polypropylene latex, and Michael Claes at Nanocyl S.A. for supplying the MWCNTs.

References and Notes

(1) Li, H.; Jiang, S.; Wang, J.; Wang, D.; Yan, S. *Macromolecules* **2003**, *36*, 2802–2807.
(2) Sandler, J.; Broza, G.; Nolte, M.; Schulte, K.; Lam, Y. M.; Shaffer, M. S. P. *J. Macromol. Sci., Phys.* **2003**, *B42*, 479–488.
(3) Zhang, S.; Minus, M. L.; Zhu, L.; Wong, C.-P.; Kumar, S. *Polymer* **2008**, in press.
(4) Bhattacharyya, A. R.; Sreekumar, T. V.; Liu, T.; Kumar, S.; Ericson, L. M.; Hauge, R. H.; Smalley, R. E. *Polymer* **2003**, *44*, 2373–2377.
(5) Moniruzzaman, M.; Winey, K. I. *Macromolecules* **2006**, *39*, 5194–5205.
(6) Iijima, S. *Nature* **1991**, *354*, 56–58.
(7) Salvetat, J. P.; Bonard, J. M.; Thomson, N. H.; Kulik, A. J.; Forro, L.; Benoit, W. *Appl. Phys., A: Mater. Sci. Process.* **1999**, *69*, 255–260.
(8) Wong, E. W.; Sheehan, P. E.; Lieber, C. M. *Science* **1997**, *277*, 1971–1975.
(9) Treacy, M. M. J.; Ebbesen, T. W.; Gibson, J. M. *Nature* **1996**, *381*, 678–680.
(10) Tans, S. J.; Devoret, M. H.; Dai, H. J.; Thess, A.; Smalley, R. E.; Geerligs, L. J. *Nature* **1997**, *386*, 474–477.
(11) Sandler, J.; Shaffer, M. S. P.; Prasse, T.; Bauhofer, W.; Schulte, K.; Windle, A. H. *Polymer* **1999**, *40*, 5967–5971.
(12) Wagner, H. D.; Lourie, O.; Feldman, Y.; Tenne, R. *Appl. Phys. Lett.* **1998**, *72*, 188–190.
(13) Wang, Y. P.; Cheng, R. L.; Liang, L. L.; Wang, Y. M. *Compos. Sci. Technol.* **2005**, *65*, 793–797.
(14) Regev, O.; ElKati, P. N. B.; Loos, J.; Koning, C. E. *Adv. Mater.* **2004**, *16*, 248–251.
(15) Gorga, R. E.; Cohen, R. E. *J. Polym. Sci., Part B: Polym. Phys.* **2004**, *42*, 2690–2702.
(16) Seo, M. K.; Park, S. J. *Chem. Phys. Lett.* **2004**, *395*, 44–48.
(17) Koganemaru, A.; Bin, Y. Z.; Agari, Y.; Matsuo, M. *Adv. Funct. Mater.* **2004**, *14*, 842–850.
(18) Thess, A.; Lee, R.; Nikolaev, P.; Dai, H. J.; Petit, P.; Robert, J. *Science* **1996**, *273*, 483–487.
(19) O'Connell, M. J.; Boul, P.; Ericson, L. M.; Huffman, C.; Wang, Y. H.; Haroz, E. *Chem. Phys. Lett.* **2001**, *342*, 265–271.
(20) Haggenmueller, R.; Gommans, H. H.; Rinzler, A. G.; Fischer, J. E.; Winey, K. I. *Chem. Phys. Lett.* **2000**, *330*, 219–225.
(21) Manchado, M. A. L.; Valentini, L.; Biagiotti, J.; Kenny, J. M. *Carbon* **2005**, *43*, 1499–1505.
(22) Potschke, P.; Bhattacharyya, A. R.; Janke, A. *Carbon* **2004**, *42*, 965–969.
(23) Cooper, C. A.; Ravich, D.; Lips, D.; Mayer, J.; Wagner, H. D. *Compos. Sci. Technol.* **2002**, *62*, 1105–1112.
(24) Jin, L.; Bower, C.; Zhou, O. *Appl. Phys. Lett.* **1998**, *73*, 1197–1199.
(25) Xu, X. J.; Thwe, M. M.; Shearwood, C.; Liao, K. *Appl. Phys. Lett.* **2002**, *81*, 2833–2835.
(26) Grossiord, N.; Loos, J.; Koning, C. E. *J. Mater. Chem.* **2005**, *15*, 2349–2352.
(27) Yu, J.; Lu, K.; Sourty, E.; Grossiord, N.; Konging, C. E.; Loos, J. *Carbon* **2007**, *45*, 2897–2903.
(28) Grossiord, N.; Loos, J.; Meuldijk, J.; Regev, O.; Miltner, H. E.; Van Mele, B.; Koning, C. E. *Compos. Sci. Technol.* **2007**, *67*, 778–782.
(29) Kimura, T.; Ago, H.; Tobita, M.; Ohshima, S.; Kyotani, M.; Yumura, M. *Adv. Mater.* **2002**, *14*, 1380–1383.
(30) Du, F. M.; Fischer, J. E.; Winey, K. I. *J. Polym. Sci., Part B: Polym. Phys.* **2003**, *41*, 3333–3338.
(31) Kumar, S.; Dang, T. D.; Arnold, F. E.; Bhattacharyya, A. R.; Min, B. G.; Zhang, X. *Macromolecules* **2002**, *35*, 9039–9043.
(32) Barraza, H. J.; Pompeo, F.; O'Rear, E. A.; Resasco, D. E. *Nano Lett.* **2002**, *2*, 797–802.
(33) Trujillo, M.; Arnal, M. L.; Müller, A. J.; Laredo, E.; Bredeau, S.; Bonduel, D.; Dubois, P. *Macromolecules* **2007**, *40*, 6268–6276.
(34) Grunlan, J. C.; Mehrabi, A. R.; Bannon, M. V.; Bahr, J. L. *Adv. Mater.* **2004**, *16*, 150–153.
(35) Dufresne, A.; Paillet, M.; Putaux, J. L.; Canet, R.; Carmona, F.; Delhaes, P. *J. Mater. Sci.* **2002**, *37*, 3915–3923.
(36) Miltner, H. E.; Grossiord, N.; Lu, K.; Loos, J.; Koning, C. E.; Van Mele, B. *Macromolecules* **2008**, *41*, 5753–5762.
(37) Li, C. Y.; Li, L. Y.; Cai, W. W.; Kodjie, S. L.; Tenneti, K. K. *Adv. Mater.* **2005**, *17*, 1198–1202.
(38) Li, L.; Yang, Y.; Yang, G.; Chen, X.; Hsiao, B. S.; Chu, B.; Spanier, J. E.; Li, C. Y. *Nano Lett.* **2006**, *6*, 1007–1012.
(39) Li, L.; Li, C. Y.; Ni, C. *J. Am. Chem. Soc.* **2006**, *128*, 1692–1699.
(40) Haggenmueller, R.; Fischer, J. E.; Winey, K. I. *Macromolecules* **2006**, *39*, 2964–2971.
(41) Grossiord, N.; Regev, O.; Loos, J.; Meuldijk, J.; Koning, C. E. *Anal. Chem.* **2005**, *77*, 5135–5139.
(42) Grady, B. P.; Pompeo, F.; Shambaugh, R. L.; Resasco, D. E. *J. Phys. Chem. B* **2002**, *106*, 5852–5858.
(43) Lieberwirth, I.; Loos, J.; Petermann, J.; Keller, A. *J. Polym. Sci., Part B: Polym. Phys.* **2000**, *38*, 1183–1187.
(44) Grossiord, N.; Miltner, H. E.; Loos, J.; Meuldijk, J.; Van Mele, B.; Koning, C. E. *Chem. Mater.* **2007**, *19*, 3787–3792.

MA8008299